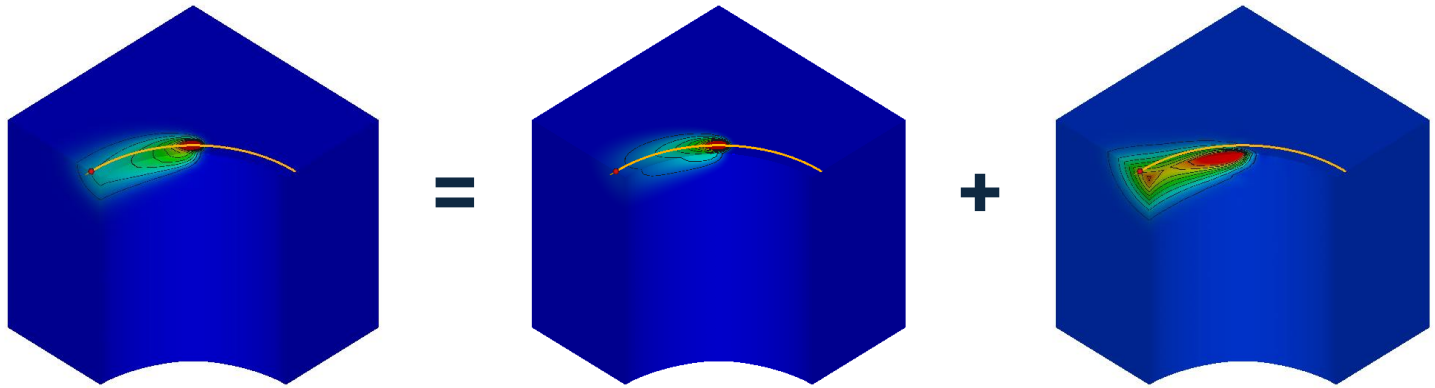
Paper: Y. Yang, Y. Ji, M. Möller, C. Ayas, CMAME 457 (2026) 118992 · open access

TU Delft Delft University of Technology

IGA 2026
Tokyo, 11–14 October 2026



A fast semi-analytical isogeometric framework for thermal problems with moving heat sources

14TH INTERNATIONAL CONFERENCE ON ISOGEOMETRIC ANALYSIS

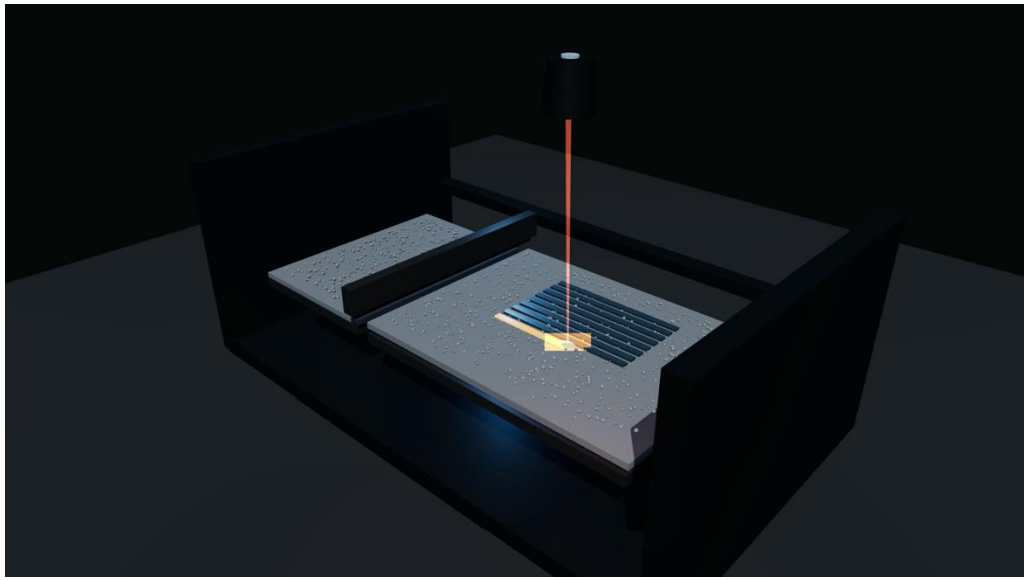
Ye Ji · **Yang Yang** · **Matthias Möller** · **Can Ayas**
Applied Mathematics & Precision and Microsystems Engineering, TU Delft
IG260030 · y.ji-1@tudelft.nl



1. Background and motivation
2. Semi-analytical IGA method
3. Numerical examples
4. Surrogates and outlook

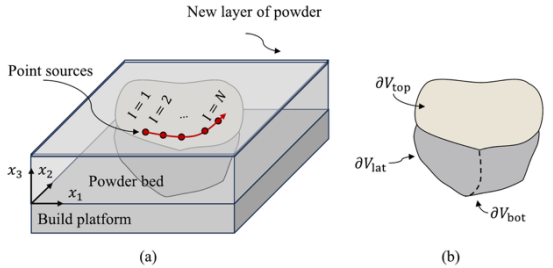
LPBF thermal simulation: a moving heat source across multiple scales

- **Laser powder bed fusion (LPBF)**, the leading metal additive manufacturing process, builds parts from powder layers 30–60 μm thick.
- The quality of lattices and topology-optimized parts depends strongly on the **temperature history**, e.g., melt pool, microstructure, residual stress, distortion.
- **Challenges**: A 20–50 μm spot moves at ~1 m/s over mm–cm parts: FEM needs **5–25 μm elements** near the laser spot, making the simulation computationally expensive even with adaptive refinement.



Recoat powder → laser scan → lower the platform → repeat.

The mesh has to resolve the laser spot along the whole scan path, although the temperature of a moving point source is known in closed form.

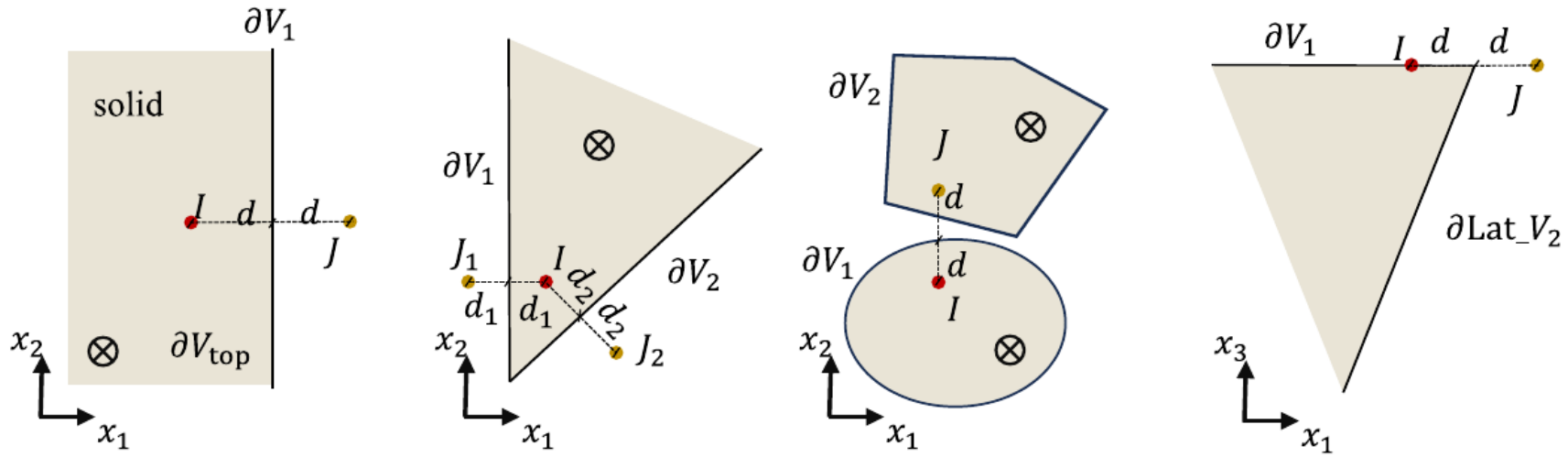


Model

scan = point sources I = 1...N; top and lateral faces adiabatic, bottom plate at T_C.

Semi-analytical models: the challenge of complex boundaries

- **Idea:** analytical point-source solution (half-space) + FE correction of the boundary conditions[1]
- **Near boundaries:** the classical FE correction needs **laser-scale refinement**; image sources[2] avoid this but need simple geometry



(a) one image J *(b) images of images* *(c) image in another solid* *(d) varying cross-section*

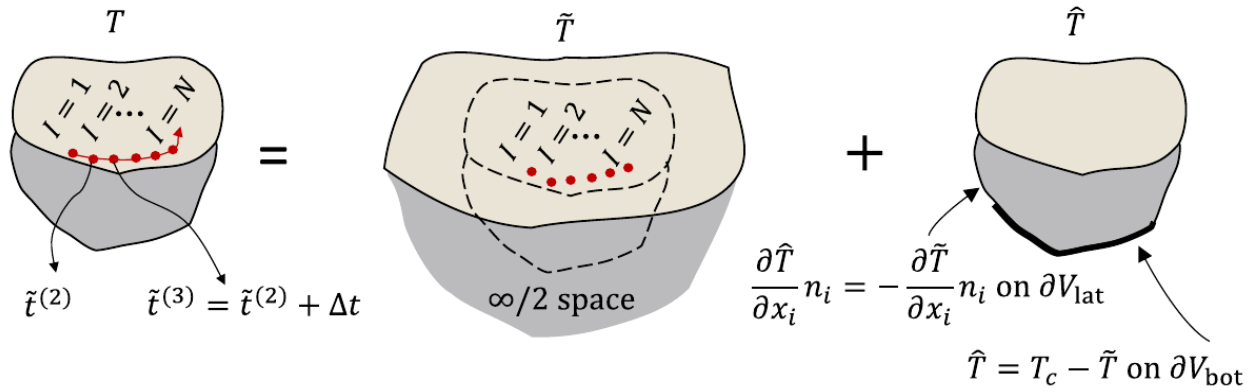
- Image sources become **difficult** to apply to **sharp corners** and **varying cross-sections**.
- How can we enforce B.C. on complex parts efficiently, without refining the mesh at the laser scale?

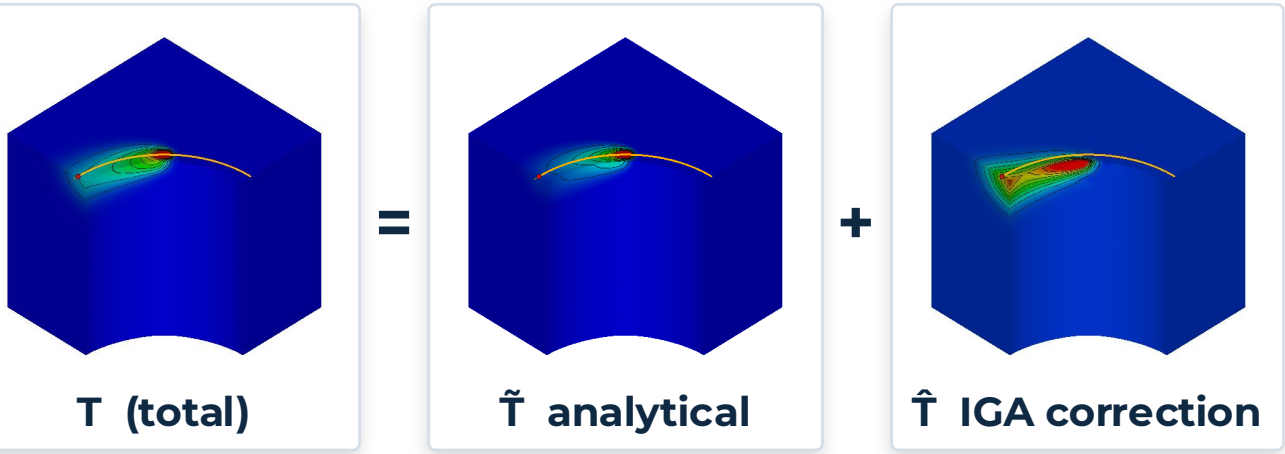
[1]Yang, Knol, van Keulen, Ayas, Addit. Manuf. 21 (2018) 284–297 [2]Yang, van Keulen, Ayas, Addit. Manuf. 31 (2020) 100955 [3]Yang, Ji, Möller, Ayas, CMAME 457 (2026) 118992



1. Background and motivation
2. Semi-analytical IGA method
3. Numerical examples
4. Surrogates and outlook

Temperature decomposition: analytical field $\tilde{T}$ + IGA correction $\hat{T}$





Contour scan, 82.5 W at 0.5 m/s; $\hat{T}$ shown on 0–400 °C.

Analytical part: point sources

$$\tilde{T}^{(I)} = \frac{E^{(I)}}{\rho c_p [4\pi\alpha(t-\tau^{(I)})]^{3/2}} \exp\left(-\frac{\|\mathbf{x}-\mathbf{x}^{(I)}\|^2}{4\alpha(t-\tau^{(I)})}\right) H(t-\tau^{(I)})$$

- E = APΔt (A: absorptivity, P: laser power), Δt = 10 μs; τ = t − r²/8α (finite spot);
- captures the laser-scale gradients **analytically**, no mesh; top surface adiabatic by construction.

B.C. Correction: smooth, on the part

$$\rho c_p \frac{\partial \hat{T}}{\partial t} = k\nabla^2 \hat{T} \quad \text{in } V$$

$$-k\frac{\partial \hat{T}}{\partial \mathbf{n}} = k\frac{\partial \tilde{T}}{\partial \mathbf{n}} \quad \text{on } \partial V_{\text{lat}} \qquad \hat{T} = T_c - \tilde{T} \quad \text{on } \partial V_{\text{bot}}$$

- cancels the analytical flux on the lateral faces, restores the bottom plate temperature;
- solved with **IGA on the exact NURBS geometry**, without resolving the laser spot in the mesh.

Spatial discretization with IGA and time integration with Crank–Nicolson

1 Weak form

$$\int_V \rho c_p \frac{\partial \hat{T}}{\partial t} w \, \mathrm{d}V + \int_V k \nabla \hat{T} \cdot \nabla w \, \mathrm{d}V = \int_{\partial V_{\mathrm{lat}}} (-q_N) \, w \, \mathrm{d}S$$

$q_N = k \, \partial \tilde{T}/\partial n$: The analytical field supplies the boundary data for the correction.

2 IGA discretization

$$\mathbf{M}\dot{\hat{\mathbf{T}}} + \mathbf{K}\hat{\mathbf{T}} = \mathbf{F}(t), \qquad \hat{T}_h = \sum_i N_i(\boldsymbol{\xi}) \, \hat{T}_i(t)$$

$M_{ij} = \int \rho c_p N_i N_j \, dV$, $K_{ij} = \int k \nabla N_i \cdot \nabla N_j \, dV$;
Dirichlet conditions imposed through the boundary coefficients.

3 Crank–Nicolson, θ = 0.5

$$\left(\frac{\mathbf{M}}{\Delta t} + \theta \mathbf{K}\right)\hat{\mathbf{T}}^{n+1} = \left(\frac{\mathbf{M}}{\Delta t} - (1-\theta)\mathbf{K}\right)\hat{\mathbf{T}}^{n} + \theta \mathbf{F}^{n+1} + (1-\theta)\mathbf{F}^{n}$$

Δt = 10 μs = one point source per step; then $T = \tilde{T} + \hat{T}$.

A fair comparison

The **same decomposition** is solved with FEM in ABAQUS:

- C3D4 linear tetrahedra
- C3D10 quadratic tetrahedra
- C3D20 quadratic hexahedra

Comparison focuses on **spatial discretization**.

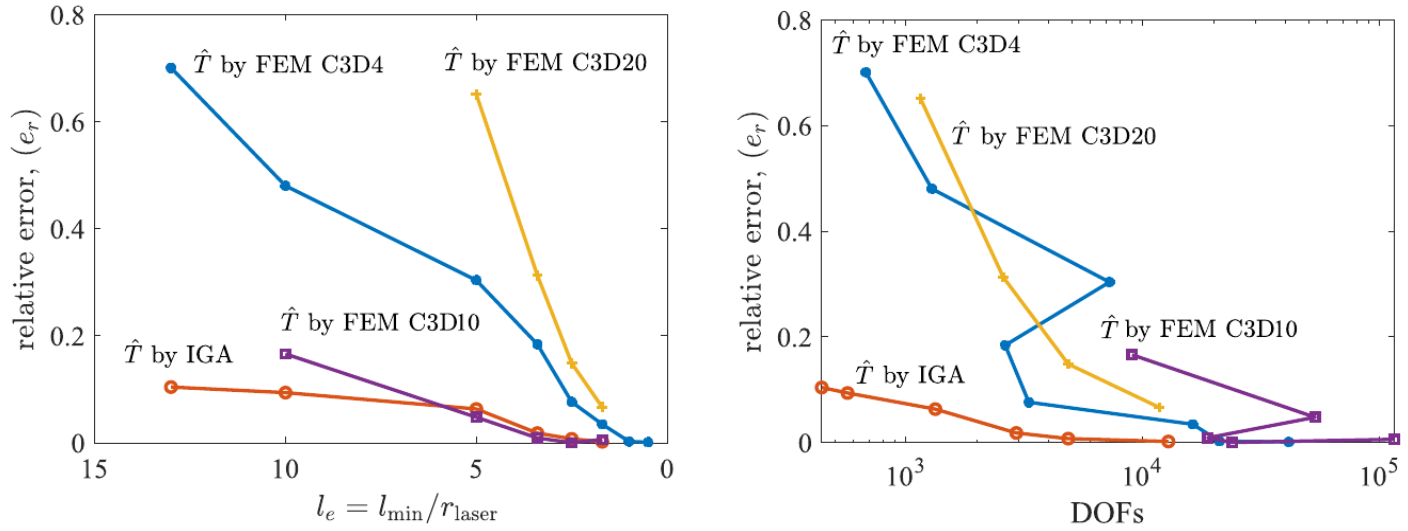
What IGA brings

- BCs on the exact geometry;
- Higher continuity within patches: smooth fluxes on coarse meshes;
- High accuracy per DOF.



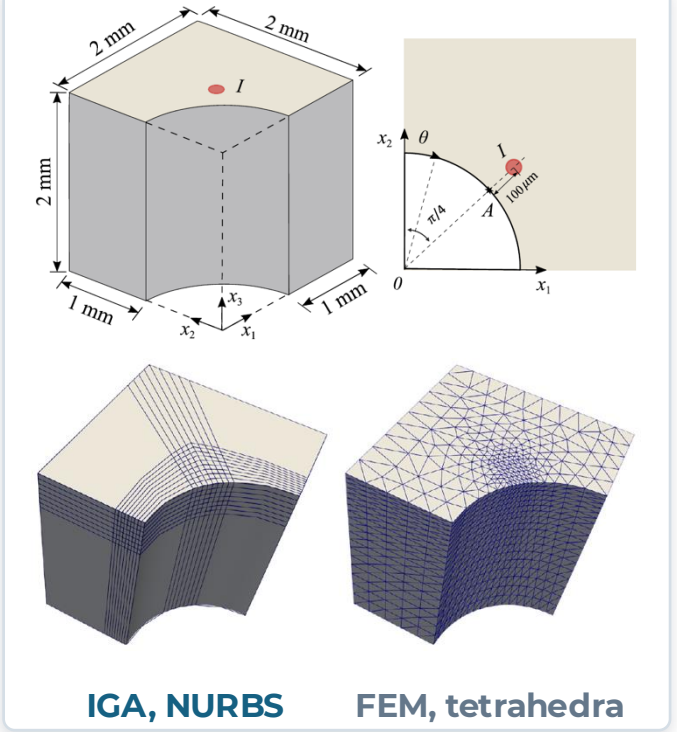
1. Background and motivation
2. Semi-analytical IGA method
3. Numerical examples
4. Surrogates and outlook

IGA resolves B.C. with elements larger than the laser spot



Relative error of $\hat{T}$ at A vs. $l_e = l_{min} / r_{laser}$ (left) and vs. DOFs (right).

Setup: Ti-6Al-4V; 82.5 W pulse, 10 µs, r = 20 µm; source **100 µm** from the arc; $\hat{T}$ at A, t = 0.19 ms (ref. FEM 5 µm: 20.79 °C).

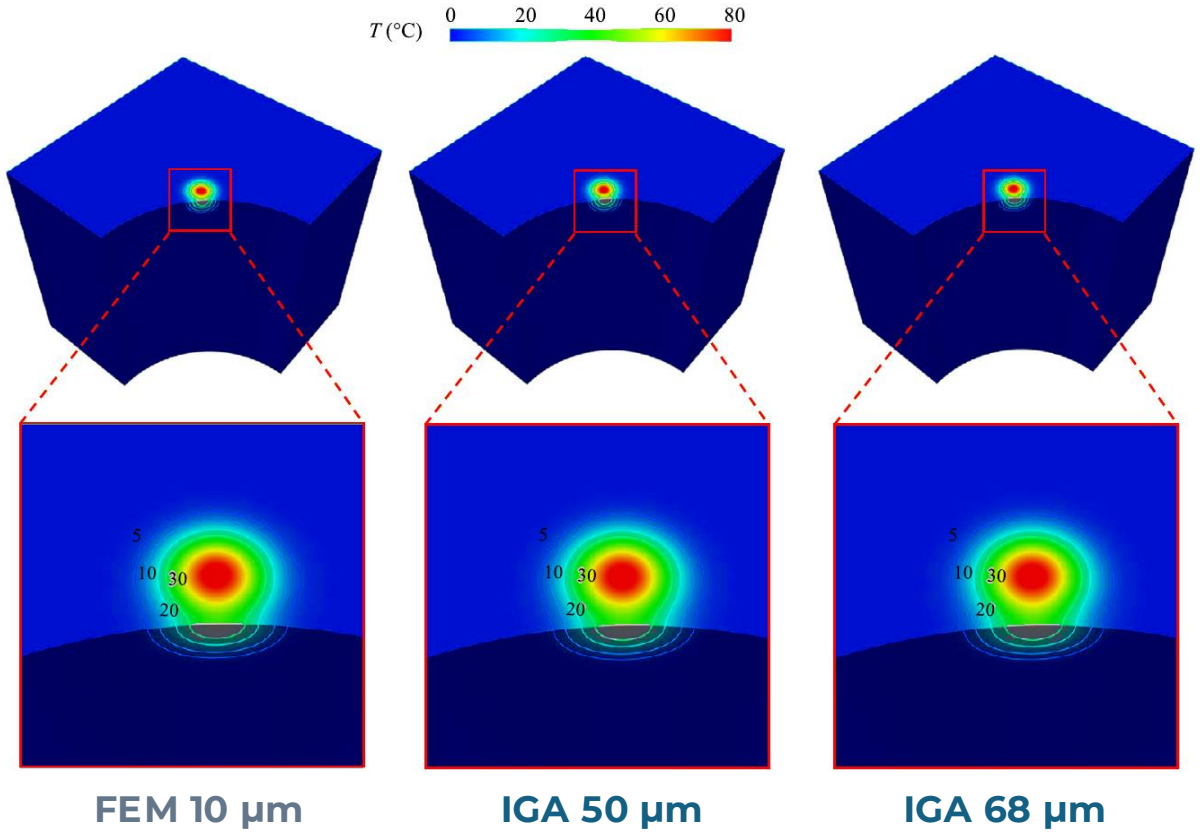


≈ 10% IGA error at **13×** the spot radius (260 µm)

< 1% IGA error at 2.5× the spot radius (50 µm)

≈ 70% linear tetrahedra at 13× the spot radius

IGA achieves a smaller boundary-flux residual with 5× larger elements



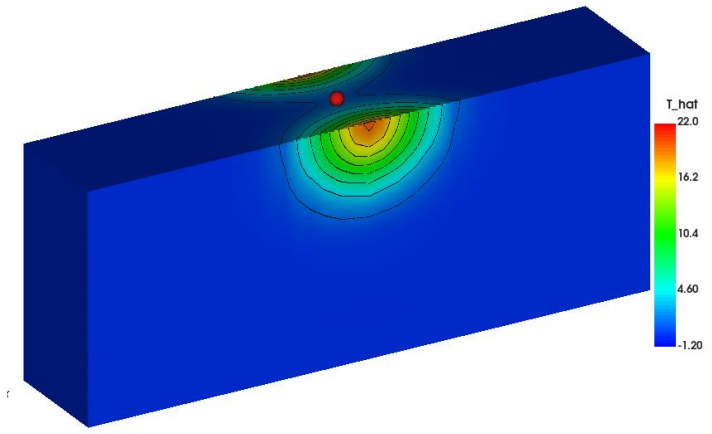
T at t = 0.19 ms; insets zoom on the source at the arc.

mesh	l_e	error at A	Relative flux residual
FEM 10 μm	0.5	0.10%	7.4%
IGA 50 μm	**2.5**	**0.73%**	**4.8%**
IGA 68 μm	3.4	1.8%	9.2%
IGA 100 μm	5.0	6.3%	27.6%

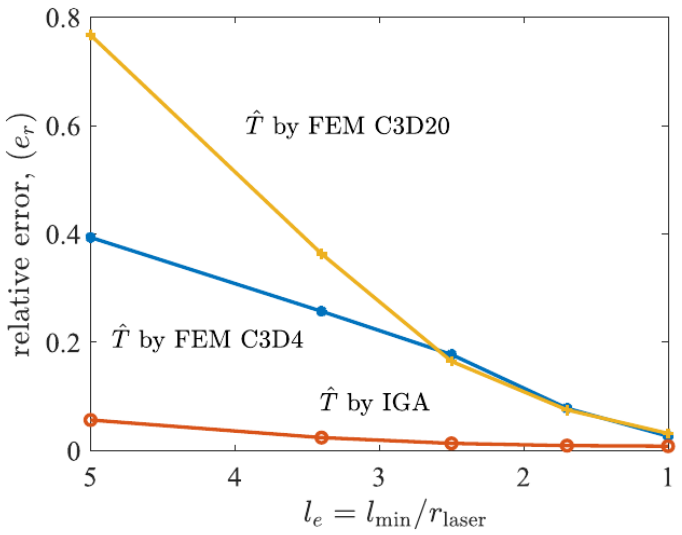
Relative flux residual = $\int|\tilde{q} + \hat{q}|\, ds / \int|\tilde{q}|\, ds$ along the boundary

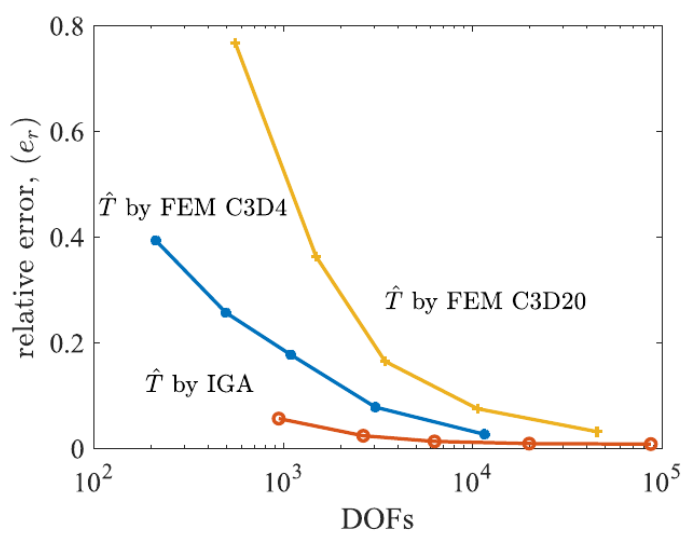
- Isotherms meet the curved boundary approximately **at right angles**, consistent with the adiabatic boundary condition
- IGA 50 μm loses **4.8%** of the flux vs 7.4% for FEM 10 μm, with 5× larger elements
- IGA 100 μm loses 27.6%: the laser heat source sits on the patch's **C^0 line**

Thin wall: IGA is 80–258× faster per time step within 5% error



One pulse: $\hat{T}$ sits at the side walls





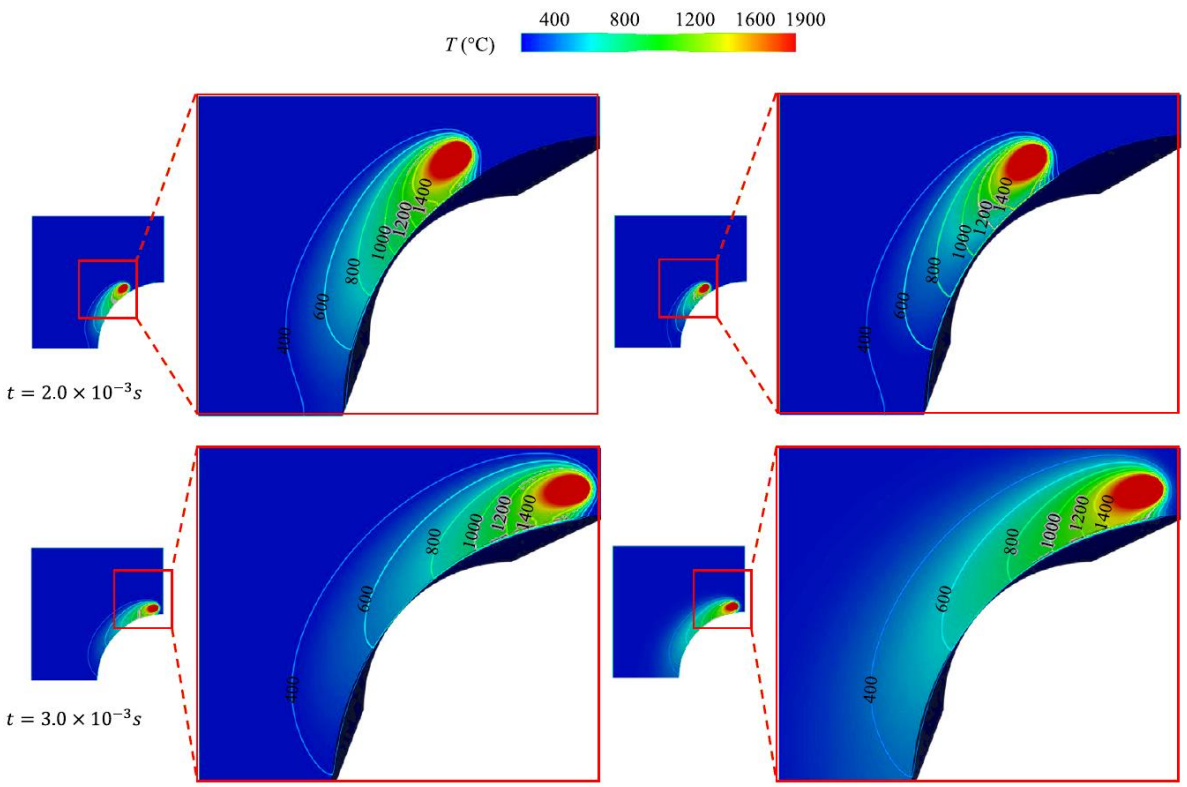
discretization	element	DOFs	time / step	Time relative to IGA
IGA, quadratic	**68 µm**	**2 639**	**0.132 s**	**1×**
FEM, C3D4 linear tet	20 µm	11 536	10.6 s	80×
FEM, C3D20 quadratic hex	—	45 261	34.0 s	258×

Uniform meshes; within 5% relative error; Intel i7-11700 @ 2.5 GHz.

4–17×

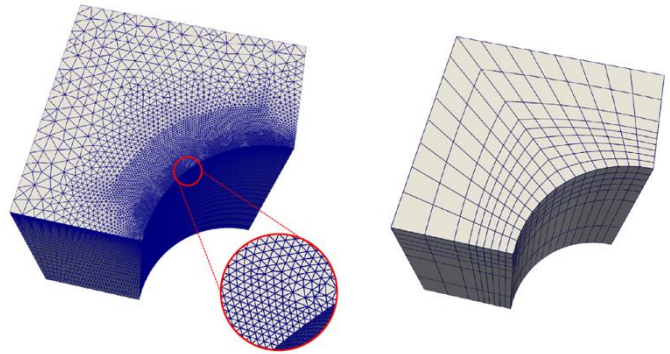
fewer DOFs at the same error tolerance: splines resolve the **through-thickness gradient**

Continuous scanning: 7× fewer DOFs and smaller boundary-flux residuals



FEM 10 µm **IGA 100 µm**

T at t = 2 ms (top) and 3 ms (bottom).

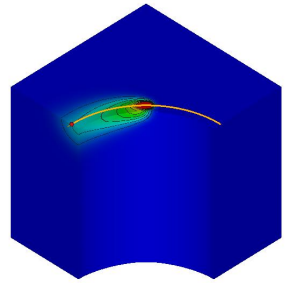


45 773
DOFs, FEM 10 µm

6 137
DOFs, IGA 100 µm

Relative flux residual	t = 2 ms	t = 3 ms
FEM 10 µm	17.8%	17.3%
IGA 100 µm	**14.9%**	**8.0%**

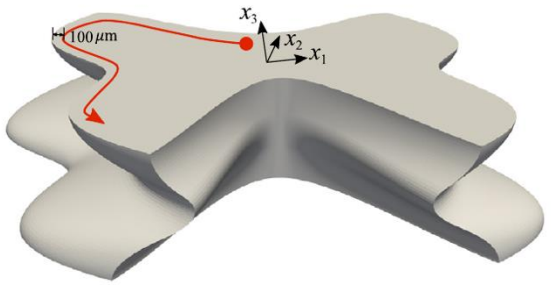
Relative flux residual as defined on slide 10; lower is better.



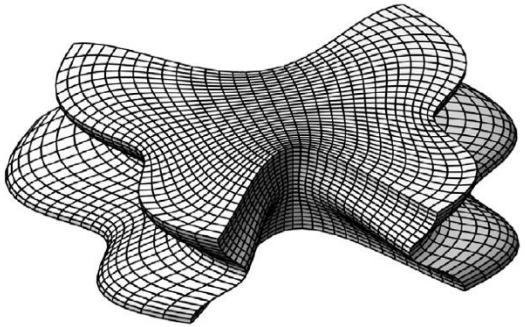
82.5 W · 0.5 m/s · 100 µm from the face

Butterfly-shaped part: extending the method to complex geometry

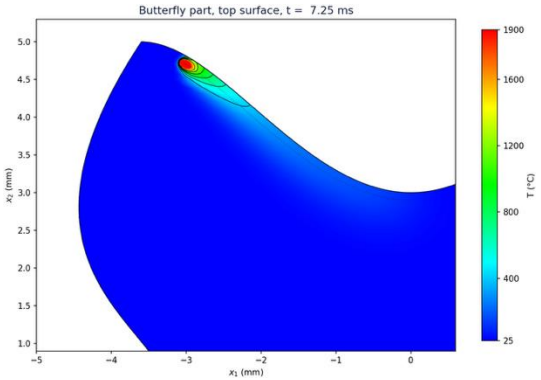
Y. Yang, Y. Ji, M. Möller, C. Ayas, CMAME 457 (2026) 118992



Geometry and scan path



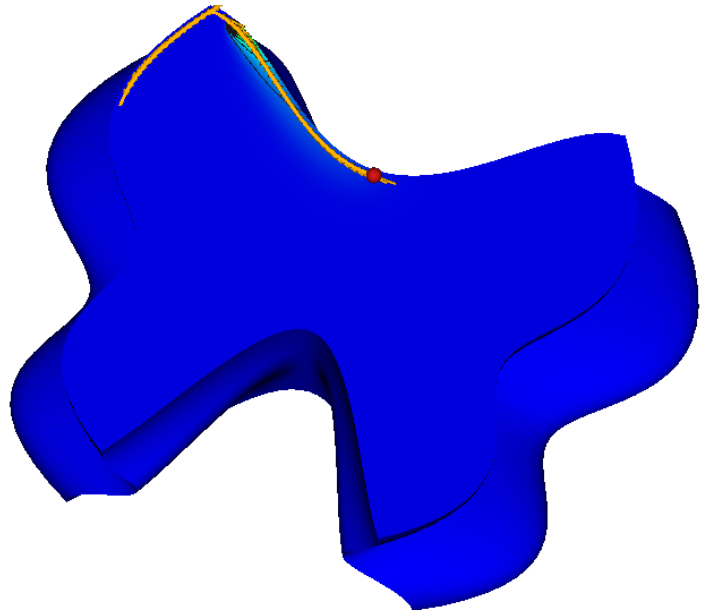
IGA parameterization



Top-surface temperature.

Setup

- Part ≈ 10 × 10 × 2 mm
- IGA: **100 μm** along the path, **27 456 DOFs**
- FEM at 10 μm: **prohibitive**
- Image sources: **not applicable**



Contour scan over the whole part, 0–12 ms.

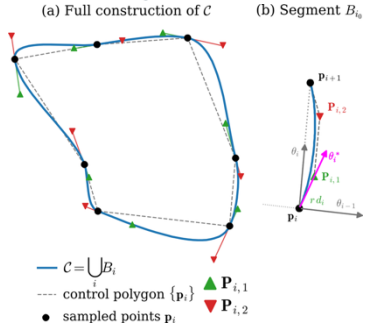
The temperature contours stay **orthogonal to every face**, consistent with the adiabatic condition on the curved and inclined boundaries.



1. Background and motivation
2. Semi-analytical IGA method
3. Numerical examples
4. Surrogates and outlook

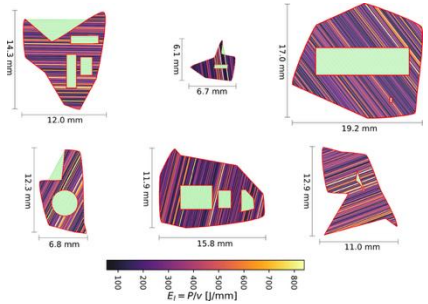
GHOST surrogate: predicting a thermal history in under 1 s

1 Random geometries



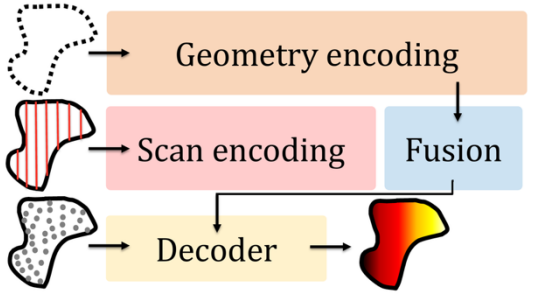
Random Bézier contours

2 2 250 semi-analytical simulations

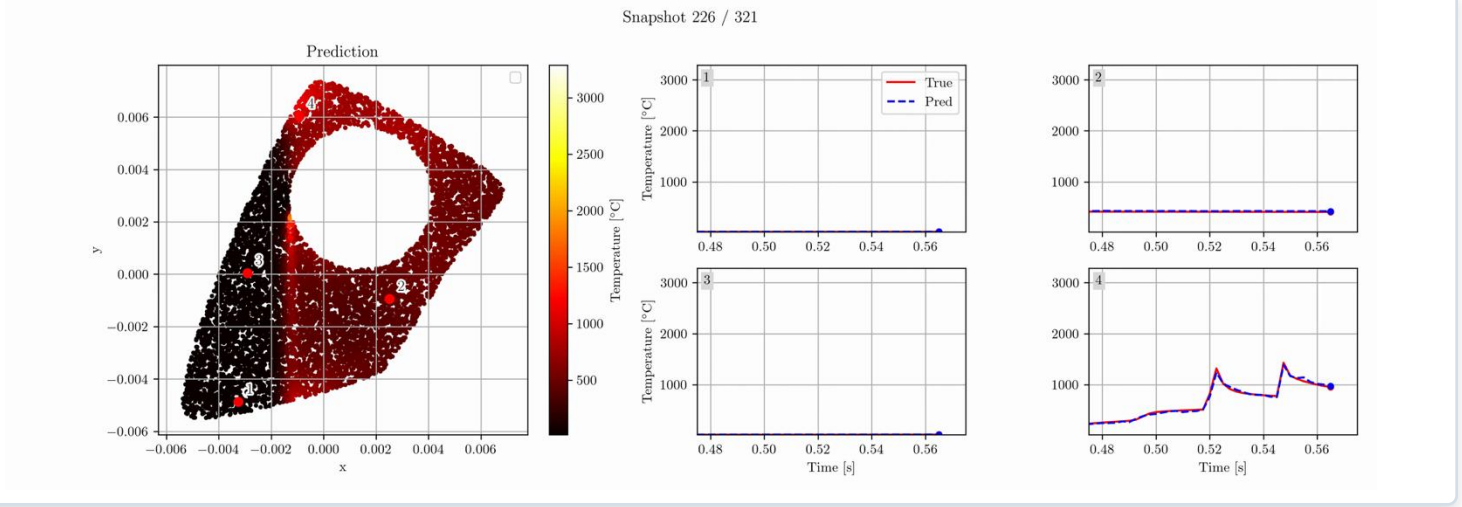


Random scans, 64 snapshots each

3 GHOST neural operator



Trained in 25 h on one A100



GHOST: Geometry-informed History-aware neural-Operator for Scan-conditioned Thermal prediction

Prediction on unseen parts

- **All queried times evaluated in parallel** in one parallel pass, no time stepping
- Unseen geometries and scans: **MAPE ≈ 5–6%** against IGA reference solutions
- **0.1–0.7 s** on a laptop GPU

Analytical heat sources + IGA boundary correction: no laser-following remeshing

Conclusions

- **Semi-analytical decomposition**: analytical heat-source solutions capture the steep temperature gradients; IGA supplies the boundary correction on the exact NURBS geometry.
- **Accuracy on coarse meshes**: the tested cases achieve accurate boundary corrections with elements larger than the laser spot, reducing the required degrees of freedom.
- **Geometric flexibility**: curved boundaries, inclined surfaces and varying cross-sections are handled without image-source constructions or laser-following remeshing.
- **Training data for surrogates**: efficient simulations across diverse geometries and scan paths support neural-operator models such as GHOST.

Outlook

- **THB adaptivity** for large parts (in progress)
- **Multi-laser** scanning
- **Experimental validation**

TU Delft Delft University of Technology

With many thanks to Felix W. Tieleman (TU Delft / NLR) for the GHOST results.

Paper: Y. Yang, Y. Ji, M. Möller, C. Ayas, CMAME 457 (2026) 118992 · open access

Many thanks for your kind attention!

Q&A

If you are interested in my research, please feel free to contact me! ;-)

- **Email:** y.ji-1@tudelft.nl
- **GitHub:** jiyess
- **Homepage:** https://jiyess.github.io/

